

Phase Equilibria in the $\text{Sb}_2\text{Te}_3\text{--InSb}$ System

V. Vassilev, L. Aljihmani, V. Milanova, and T. Hristova-Vasileva

(Submitted July 1, 2015; in revised form February 23, 2016; published online May 13, 2016)

The phase diagram of the $(\text{Sb}_2\text{Te}_3)_{100-x}\text{--InSb}_x$ system was determined based on x-ray diffraction (XRD) analysis, differential thermal analysis (DTA), and microhardness and density measurements. An intermediate compound with composition $\text{Sb}_2\text{Te}_3\cdot 2\text{InSb}$ was formed as a result of syntectic reaction, melting incongruently at 553 °C. This compound has tetragonal lattice with unit cell parameters of $a = 4.3937 \text{ \AA}$, $b = 4.2035 \text{ \AA}$, $c = 3.5433 \text{ \AA}$, $\alpha = 93.354^\circ$, and $\beta = \gamma = 90^\circ$. $\text{Sb}_2\text{Te}_3\cdot(2 + \delta)\text{InSb}$ ($-1 \leq \delta \leq +1$) and $(\text{Sb}_2\text{Te}_3)_{100-x}(\text{InSb})_x$ ($90 \leq x \leq 100$) solid solutions exist in the investigated system, based on the intermediate compound $\text{Sb}_2\text{Te}_3\cdot 2\text{InSb}$ and on InSb, respectively. Also, two invariant equilibria exist in the system, with eutectic point coordinates at compositions of $x = 60$ and $x \approx 85 \text{ mol\% InSb}$ and eutectic temperatures of $T_E = 541$ and $T_E = 501 \text{ }^\circ\text{C}$, respectively.

Keywords differential thermal analysis, phase diagram, phase equilibria, solid solution, X-ray analysis

1. Introduction

Identification of new energy sources is currently a focus of scientific endeavor. Such investigations aim to develop new, highly effective technologies for energy transformation, especially based on nonmechanical, direct energy conversion to electricity. One direction to address this aim is use of thermoelectric, thermoemission, and magnetic hydrodynamic transformation of heat energy to electricity, among which the thermoelectric method is the most well developed. In parallel with such development of new methods and technologies for transformation of a given kind of energy to electricity, researchers are also working on the discovery, development, and introduction of new, highly effective thermoelectric materials.

Many requirements have to be fulfilled by effective thermoelectric materials. One of the most important is to possess high thermoelectric efficiency coefficient (Z), also known as the Ioffe criterion^[1,2]:

$$Z = \alpha^2 \sigma / \lambda, \quad (\text{Eq } 1)$$

V. Vassilev, Department of Non-Ferrous Metals Metallurgy and Semiconductor Technologies, University of Chemical Technology and Metallurgy, 8 Kliment Ohridski blvd., 1756 Sofia, Bulgaria; and zh.k. Mladost 1A, bl. 512, entr. 2, apt. 30, 1729 Sofia, Bulgaria; L. Aljihmani and V. Milanova, Department of Non-Ferrous Metals Metallurgy and Semiconductor Technologies, University of Chemical Technology and Metallurgy, 8 Kliment Ohridski blvd., 1756 Sofia, Bulgaria; and T. Hristova-Vasileva, Georgi Nadjakov Institute of Solid State Physics, Bulgarian Academy of Sciences, 72 Tzarigradsko Chaussee blvd., 1784 Sofia, Bulgaria. Contact e-mails: l_aljihmani@abv.bg and venci_vassilev@abv.bg.

where α is the thermoelectromotive force (TEMF), σ is the specific electrical conductivity, and λ is the thermal conductivity coefficient.

In order to increase the thermoelectric efficiency coefficient, researchers are mainly working in two directions:

- Improvement of the properties of materials already approved and used in practice, using various methods including compositional and structural variation of the initial material, doping, substitution in one or both sublattices, external impacts (thermal, electrical, optical, magnetic, supersonic), etc.
- Development of new thermoelectric materials with appropriate properties and high Z values

In both cases, the final goal is:

- Optimization of charge-carrier concentration, i.e., electrons (n) or holes (p), and widening of the working interval
- Adjustment of the ratio between the mobilities of the charge carriers μ_n and μ_p (i.e., μ_n/μ_p), as well as the ratio between the effective mass of electrons m_n and holes m_p (i.e., m_n/m_p), etc.

Such changes lead to new values of the three parameters α , σ , and λ , which should guarantee higher Z values compared with the initial (conventional) thermoelectric material or production of new material with higher Z values and wider working temperature interval.

Calculations have shown that the maximum value of $\alpha^2 \sigma$ is achieved in the concentration limit $n(p) = 3 \times 10^{18} \text{--} 3 \times 10^{19} \text{ cm}^{-3}$. This means that up to $3 \times 10^{19} \text{ cm}^{-3}$ dopants must be dissolved in the thermoelectric material.^[3]

The maximal value of the thermoelectric efficiency coefficient Z is obtained at $\alpha = 2(k/e) \cong 172 \text{ } \mu\text{V/K}$, when neglecting the influence of the concentration of charge carriers $n(p)$ on their mobility (μ) and on the thermal conductivity coefficient λ .^[4]

The thermal conductivity coefficient (λ) directly influences the Z value. Since for most semiconductor thermoelectric materials the phonon part of the thermal conductivity (λ_{ph}) is much larger than the electronic one (λ_e), a decrease of λ_{ph} will lead to an increase of α [$\alpha = 172(1 + \lambda_e/\lambda_{ph})$] and thereby Z . An extremely efficient way to decrease λ_{ph} is through the formation of solid solutions, where additional effective centers for phonon and electron scattering are created. In the case of solid solutions, the decrease of λ_{ph} is greater than that of μ , leading to an increase in the μ/λ_{ph} ratio and thereby Z .

Since the optimal charge-carrier concentration depends strongly on temperature (as $T^{3/2}$), the $Z(T)$ dependence is characterized by a maximum. The maximal temperature (T_{max}), at which $Z = Z_{max}$, depends on the bandgap ΔE . This effect limits the working temperature of already known thermoelectric materials and can be determined using

$$\sigma k T_{max} = \Delta E, \quad (\text{Eq 2})$$

where k is the Boltzmann constant.

The relation between Z_{max} and ΔE is

$$Z_{max} = (r + 2 + \Delta E/2kT)^2 / (r + 2 + T), \quad (\text{Eq 3})$$

where r is a coefficient characterizing the scattering mechanism of the charge carriers.

A reasonable solution is a bandgap that is 4–6 times larger than the thermal energy (kT) at the maximal working temperature;^[5] i.e., if T_{max} is the temperature of the hot junction, then

$$4kT_{max} \leq \Delta E \leq 6kT_{max}. \quad (\text{Eq 4})$$

It can be easily calculated from Eq 4 that materials with a bandgap within the range of $\Delta E = 0.10$ – 0.15 eV (at 300 K), $\Delta E = 0.28$ – 0.41 eV (at 800 K), and $\Delta E = 0.10$ – 0.15 eV (at 1300 K) should have maximum thermoelectric efficiency.

As mentioned above, development of highly effective materials is attempted in two directions, namely improvement of the properties of conventional materials using a variety of approaches and methods, and development of completely new materials using the advanced achievements of contemporary technologies. In both cases, such investigation follows the same scheme:

synthesis \rightarrow structure \rightarrow properties \rightarrow application.

The first stage necessarily involves study of the phase equilibria and building the phase diagram of the corresponding binary, ternary, or more complicated system. In this work, we studied the development of new thermoelectric materials by modification of the classic material Sb_2Te_3 with InSb. The first step is evaluation of the phase diagram of the Sb_2Te_3 –InSb system. Knowledge of the form of this phase diagram answers the question of whether any solid-solution regions or intermediate compounds with or without homogeneity regions exist in this system.

In previous investigations into the phase equilibria in binary systems including Sb_2Te_3 (of the Sb_2Te_3 – Me_nCh_m

kind), it has been established that solid solutions based on Sb_2Te_3 as well as on its compounds are obtained. Ikeda et al.^[6,7] and Shelimova et al.^[8] investigated the PbTe– Sb_2Te_3 system. Tompson et al.^[9] performed investigations on alloys from the GeTe–AgSbTe₂ system, in which the ternary compound is an intermediate compound in the Ag_2Te – Sb_2Te_3 system, etc. Presence of both solid solutions and intermediate compounds (PbSb₂Te₄, PbSb₄Te₇, AgSbTe₂, etc.) was found in these systems.

The next stage in the scheme proposed above is detailed investigation on such materials' structure and properties, as well as determination of possible applications of the solid solutions and intermediate compounds; For example, teams led by Shelimova,^[10,11] Nemov,^[12] and Zhitinskaya^[13] investigated the two new phases PbSb₂Te₄ and PbSb₄Te₇ with the aim of obtaining monocrystals and investigating their structure, the anisotropy of their thermoelectric properties, Nernst–Ettingshausen and Hall effects, etc. Ikeda et al.^[14] reported the presence of another intermediate metastable compound in the PbTe– Sb_2Te_3 system with composition Pb₂Sb₆Te₁₁, whose microstructure is built from nanosized lamellae of PbTe and Sb_2Te_3 separated by an epitaxially similar surface.

Other approaches to development of new, more effective thermoelectric materials should not be underestimated. Such materials include doped solid solutions and compounds with thermoelectric properties (for example, PbSb₂Te₄ with Cd, Ag, and Te^[15]) or their complex compositions (multicomponent systems with at least two components with thermoelectric properties, for example, the Bi₂Te₃– Sb_2Te_3 –Zn₄Sb₃ system^[16]).

Based on the above discussion, our aim is to investigate and develop new thermoelectric materials in the Sb_2Te_3 –InSb system.

The base compound Sb_2Te_3 belongs to the group of low-temperature thermoelectric materials, operating in the temperature range of 0–300 °C.

In the Sb–Te system, one chemical compound (Sb_2Te_3) is formed, which melts with open maximum at 622 °C^[17] and has three phases (solid solutions) α , β , and γ , localized in the concentration regions of 0.0–0.8, 17.3–36.9, and 40.9–53.8 at.% Te, respectively.^[18]

Sb_2Te_3 has a rhombohedral lattice of tetradymite type, based on nine-layered packing of Te atoms, with 2/3 of octahedral sites occupied by Sb atoms. The layers are placed in accordance with the cubic packing law.^[19] The rhombohedral lattice of tetradymite type can be considered as a hexagonal layered structure, in which the unit cell contains 15 atoms, grouped in three “quintuple” layers Te¹–Sb–Te²–Sb–Te¹ and placed one above each other. The subscripts “1” and “2” indicate that the Te atoms take different positions in the crystalline lattice. The unit cell parameters of the hexagonal Sb_2Te_3 structure are $a = b = 4.264$ Å, $c = 30.458$ Å, $\alpha = \beta = 90^\circ$, and $\gamma = 120^\circ$.^[20]

The thermal bandgap of Sb_2Te_3 is 0.19 eV.^[21] It always shows p -type conductivity with high charge-carrier concentration of 10^{19} – 10^{20} cm⁻³.^[22,23] There are no data regarding change of the conductivity type to negative.

The electrical conductivity of Sb_2Te_3 at 300 K depends on the charge-carrier concentration and varies in the range of 2000–

4000 S/cm.^[22,24] Samples with stoichiometric ratio between the components show the minimal electrical conductivity value.

The values of the thermal conductivity coefficient and TEMF for Sb_2Te_3 at 300 K are 3.2×10^{-2} W/(cm K) and $+80$ – 100 $\mu\text{V/K}$,^[4] respectively.

One compound (InSb) is formed in the In–Sb phase diagram, melting congruently at 536 °C.^[25,26] A degenerate eutectic is observed on the In side. An extremely narrow homogeneity region around the InSb compound is observed on the microdiagram of the In–Sb system. The InSb compound crystallizes in a sphalerite-type lattice with unit cell parameter $a = 6.479$ Å.^[27,28]

InSb is a narrow-gap semiconductor with $\Delta E_0 = 0.27$ eV^[29] at 0 K and 0.18 eV at 300 K.^[30]

The electrical conductivity (σ) of InSb changes over a wide range depending on the concentration of impurities. σ varies around 10^{-1} – 10^2 S/cm in the low-temperature region, but in practice does not depend on temperature.^[30] At $T > 300$ K, an increase of σ with temperature and impurity concentration is observed, reaching values of about 3000 S/cm at 900 K.^[31]

InSb is characterized by high α values at low temperatures, especially for samples with p -type conductivity. Under these conditions, the hole TEMF reaches values of $\alpha_p = +770$ $\mu\text{V/K}$.^[31,32] For temperature of 300 K, the reported values are $+335$ $\mu\text{V/K}$ ^[31] and 365 $\mu\text{V/K}$.^[33]

For InSb, the temperature dependence of the thermal conductivity coefficient (λ) is characterized by a minimum at room temperature (T_r). The λ value is mainly influenced by the phonon (λ_{ph}) and electron (λ_e) contributions ($\lambda \approx \lambda_{\text{ph}} + \lambda_e$), so the observed minimum must be related to the dominant influence of λ_{ph} or λ_e . In the present case, λ_{ph} ($\lambda_{\text{ph}} \sim 1/T$) is dominant at $T < T_{\text{room}}$, while at $T > T_{\text{room}}$, λ_e becomes dominant ($\lambda_e = LT\sigma$, where L is the Lorenz number). λ_{ph} and λ_e are 0.17 and 0.01 W/(cm K), respectively, at the temperature corresponding to Z_{max} .^[34]

The aim of the present investigation is to build the phase diagram of the Sb_2Te_3 –InSb system on the basis of experimental results obtained from differential thermal analysis (DTA) and x-ray diffraction (XRD) analysis, as well as measurements of the main physicochemical properties of the samples (phase-transformation temperatures, density d , and microhardness H_V).

2. Materials and Methods

The $(\text{Sb}_2\text{Te}_3)_{1-x}(\text{InSb})_x$ system, where x is the molar percentage of InSb, was studied using 17 compositions in the concentration interval of 0–100 mol% InSb. The samples were obtained by direct monotemperature synthesis (stepwise heating at temperatures of 500 and 700 °C for 0.5 and 2 h, respectively) of Sb_2Te_3 and InSb mixed in appropriate quantities in vacuum and sealed in quartz ampoules under residual pressure of ~ 0.1 Pa. The initial compounds Sb_2Te_3 and InSb were synthesized using the same method from initial elements of purity 4 N (Sb) or 5 N (In, Te). Vibration stirring of the melt was applied, followed by cooling with the furnace turned off.

DTA and XRD analysis were performed at least 180–200 h after the end of the synthesis procedures.

The phase transformations in the samples were investigated by means of DTA (Paulik–Paulik–Erdey equipment made by MOM, Hungary) at heating rate of 10 °C/min. The reference substance (calcinated $\gamma\text{-Al}_2\text{O}_3$) and the studied substance (0.5 g) were placed in special tubes (Stepanov vessels) which were then vacuum sealed under pressure of 0.133 Pa. The accuracy of the DTA measurements was ≤ 5 °C.

XRD measurements were carried out using an x-ray powder diffractometer (D2 Phaser Bruker AXS) with Cu K_α radiation and Ni filter in the Bragg angle range of $2\theta = 5$ – 90° .

The Vickers microhardness, H_V , was determined using a MIM-7 microscope with built-in microhardness meter (PMT-3) at load of 10 g. The final H_V values were obtained as averages of 100 measurements on each sample (accuracy ≤ 4 %).

Sample density (d) was evaluated by the hydrostatic method using toluene as immersion fluid. Final density values were obtained as averages of 20 measurements on different pieces of each sample (accuracy ≤ 3 %).

3. Results and Discussion

The results of XRD analysis are presented in Fig. 1.

The x-ray analysis data of the initial components (Sb_2Te_3 and InSb) coincide with those published in Ref 35 and 36, respectively.

In the concentration interval of $25 < x < 90$ mol% InSb, the distinct appearance of new lines is observed, differing from those of Sb_2Te_3 and InSb, with maximal intensity and “purity” of the peaks for the composition containing 66.7 mol% InSb. This indicates the existence of an intermediate phase with probable composition $\text{Sb}_2\text{Te}_3\cdot 2\text{InSb}$. In the concentration interval of $66.7 \leq x \leq 75.0$, the diffraction

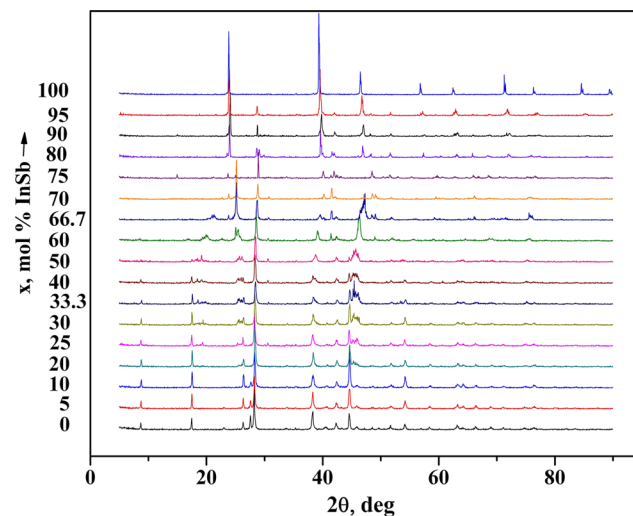


Fig. 1 XRD patterns for the Sb_2Te_3 –InSb system

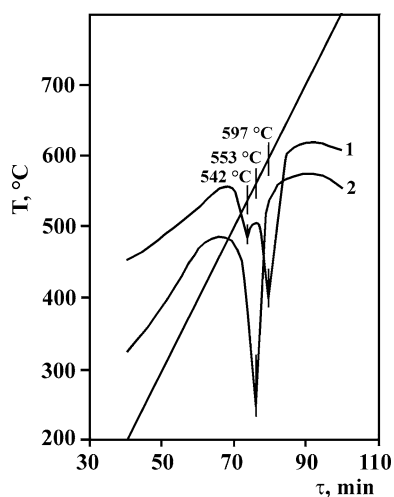


Fig. 2 Typical thermograms of samples from the $(\text{Sb}_2\text{Te}_3)_{1-x}(\text{InSb})_x$ system for (1) $x = 30$ mol% InSb and (2) $x = 66.7$ mol% InSb

reflexes of this compound shifted towards higher Bragg angle (θ), while in the concentration interval of $66.7 \geq x \geq 50.0$, they shifted towards lower angle (Fig. 1). This behavior indicates that the $\text{Sb}_2\text{Te}_3 \cdot 2\text{InSb}$ compound has variable composition of $\text{Sb}_2\text{Te}_3 \cdot (2 + \delta)\text{InSb}$ ($-1 \leq \delta \leq +1$), with a homogeneity region of 50–75 mol% InSb.

Shift of the InSb reflections towards higher θ is observed in the concentration interval of $100 \geq x \geq 90$, providing evidence for the existence of limited solid solutions based on InSb.

The diffraction reflexes of the intermediate compound $\text{Sb}_2\text{Te}_3 \cdot 2\text{InSb}$ are found in the concentration intervals of $20 \leq x < 50$ mol% InSb (I) and $75 < x < 90$ mol% InSb (II), and their intensity decreases with increasing content of Sb_2Te_3 (in region I) or InSb (in region II), respectively.

The phase-transition temperatures were determined from the heating curves and the thermal effects observed in DTA patterns (thermograms). Typical thermograms are shown in Fig. 2, and the results of this analysis are presented in Table 1.

All effects registered in the DTA patterns were endothermal. The most clearly observed (with a few exceptions) are the effects from column 4 of Table 1 (sharp peak and large area), corresponding to the liquidus line. The thermal effects in the concentration interval of 60–80 mol% InSb are relatively weak, which is typical for systems showing lamination tendency in liquid state (systems with monotectic, monotectoidal, or syntectic invariant equilibria, as well as systems with binodal curve).

Three groups of endothermal effects exist in the investigated system (Table 1), at temperatures independent of the sample composition. These are the effects from columns 1 and 2. Such a form of the temperature–concentration dependence proves the presence of different invariant equilibria or solid-state transformations. The temperatures of the effects in column 3 depend on composition, which is typical for solidus and liquidus lines.

Table 1 Temperatures of endothermal effects recorded on DTA curves of investigated samples

| No. | Composition (x mol% InSb) | Endothermal effect, °C | | | |
|-----|---------------------------|------------------------|-----|-----|-----|
| | | 1 | 2 | 3 | 4 |
| 1 | 0 | ... | ... | ... | 620 |
| 2 | 5 | ... | ... | ... | 617 |
| 3 | 10 | 542 | ... | ... | 616 |
| 4 | 20 | 544 | ... | ... | 611 |
| 5 | 25 | 542 | ... | ... | 603 |
| 6 | 30 | 542 | ... | ... | 597 |
| 7 | 33.3 | 539 | ... | ... | 597 |
| 8 | 40 | 540 | ... | ... | 577 |
| 9 | 50 | 541 | ... | ... | 549 |
| 10 | 60 | 542 | ... | ... | 541 |
| 11 | 66.7 | ... | 553 | ... | ... |
| 12 | 70 | ... | 553 | ... | 568 |
| 13 | 75 | ... | 552 | ... | 570 |
| 14 | 80 | 498 | ... | ... | 539 |
| 15 | 90 | 501 | ... | 501 | 522 |
| 16 | 95 | ... | ... | 510 | ... |
| 17 | 100 | ... | ... | 529 | 529 |

Because of the impossibility of revealing the microstructure of the different phases of the samples by selective chemical etching due to the similarity of the chemical properties of Sb_2Te_3 and InSb, a statistical approach was adopted, according to which the number of phases is evaluated based on microhardness values. One hundred measurements were performed for each sample, and the obtained H_V values were grouped by similarity; the number of groups then reveals the number of phases. The H_V values for each phase were then averaged.

The concentration dependence of the microhardness (H_V) and density (d) is shown in Fig. 3 and 4, respectively.

The following conclusions can be made from the analysis of the $H_V(x)$ dependence:

- There are four concentration regions in the microhardness–composition diagram (Fig. 3). The samples are two-phase (two H_V values) in two of them ($0 < x < 50$ and $75 < x < 90$ mol% InSb), while in the other two ($50 \leq x \leq 75$ and $90 \leq x \leq 100$ mol% InSb), the samples are monophasic (one H_V value).
- The $H_V(x)$ dependence in the monophasic regions is characterized by negative convexity, providing qualitative evidence for the existence of a homogeneity (solid-solution) region. A singular point, albeit weakly expressed, is observed at $x = 66.7$ mol% InSb in the $H_V(x)$ dependence in the concentration interval of $50 \leq x \leq 75$ mol% InSb. This is related to the existence of an intermediate phase or compound (in the current case, an intermediate compound with composition $\text{Sb}_2\text{Te}_3 \cdot 2\text{InSb}$). On the left and right of this composition, the $H_V(x)$ dependence maintains its smooth path with negative convexity. This variation of $H_V(x)$ confirms the presence of two homogeneity subareas, i.e.,

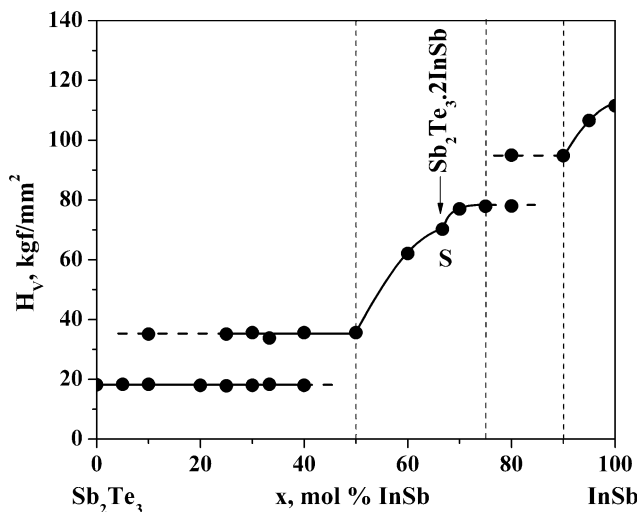


Fig. 3 $H_V(x)$ dependence of samples from the Sb_2Te_3 -InSb system

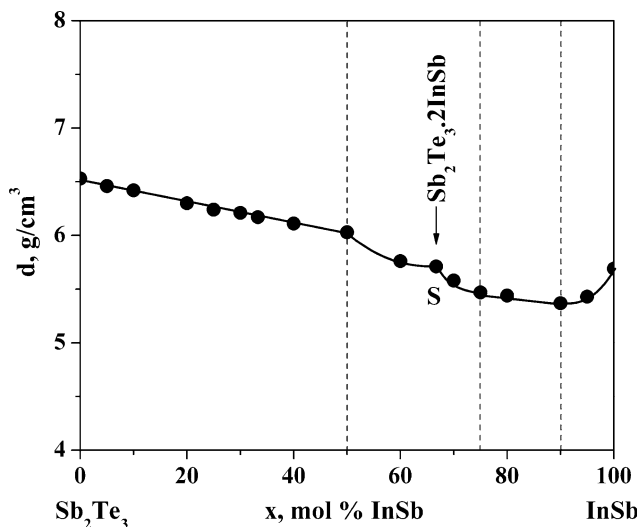


Fig. 4 $d(x)$ dependence of samples from the Sb_2Te_3 -InSb system

solid solutions based on $\text{Sb}_2\text{Te}_3 \cdot 2\text{InSb}$ or $\text{Sb}_2\text{Te}_3 \cdot (2 + \delta)\text{InSb}$ ($-1 \leq \delta \leq +1$). Limited solid solutions, based on InSb, exist in the concentration interval of $90 \leq x \leq 100$ mol% InSb. Evidence for this is provided by the smooth variation in the $H_V(x)$ dependence.

- The Vickers microhardness of the investigated samples varied between 18 and 112 kgf/mm². For the initial components Sb_2Te_3 and InSb, the values are 18 kgf/mm²^[37] and 220 kgf/mm²^[33] respectively. The microhardness of the intermediate phase is 70 ± 3 kgf/mm².

The density values (d) of the samples from the Sb_2Te_3 -InSb system (Fig. 4) fall between the density values of the

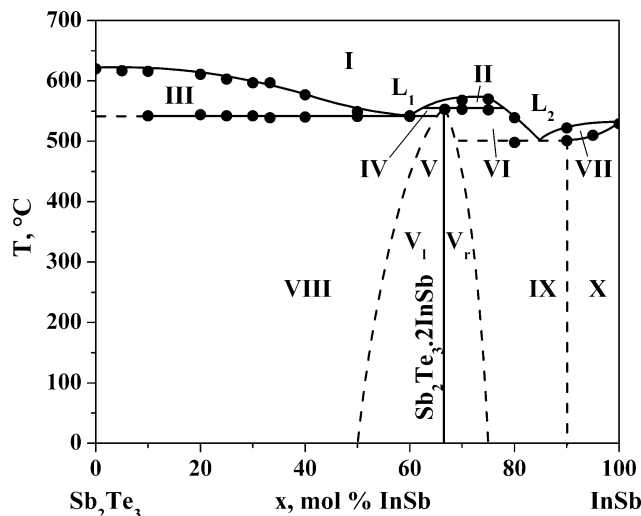


Fig. 5 Phase diagram of the Sb_2Te_3 -InSb system; I—liquid (melt—L); II— $L_1 + L_2$; III— $\text{Sb}_2\text{Te}_3 + L_1$; IV— $L_1 + \text{Sb}_2\text{Te}_3 \cdot (2 + \delta)\text{InSb}$; V— $\text{Sb}_2\text{Te}_3 \cdot (2 + \delta)\text{InSb}$ (solid solution); V_r —solid solution, rich in InSb; VI— $\text{Sb}_2\text{Te}_3 \cdot (2 + \delta)\text{InSb} + L_2$; VII— $L_2 + \alpha\text{-InSb}$; VIII— $\text{Sb}_2\text{Te}_3 + \text{Sb}_2\text{Te}_3 \cdot (2 + \delta)\text{InSb}$; IX— $\text{Sb}_2\text{Te}_3 \cdot (2 + \delta)\text{InSb} + \alpha\text{-InSb}$; X— $\alpha\text{-InSb}$ (solid solution)

initial components Sb_2Te_3 (6.5 g/cm³)^[38] and InSb (5.775 g/cm³)^[38]. The density of the intermediate compound $\text{Sb}_2\text{Te}_3 \cdot 2\text{InSb}$ is 5.71 g/cm³.

Four areas were observed in the concentration–density dependence (Fig. 4), showing the following peculiarities:

- The $d(x)$ dependence is linear in two concentration ranges ($0 \leq \delta \leq 50$ and $75 \leq \delta \leq 90$ mol% InSb); i.e., the samples in these areas are two-phase.
- The samples in the interval $90 \leq x \leq 100$ mol% InSb are monophasic, since the $d(x)$ dependence shows positive convexity in this range. In the interval $50 \leq x \leq 75$ mol% InSb, the $d(x)$ dependence is divided into two parts by the point S (singular point). The singular point appears at composition $x = 66.67$ mol% InSb and is related to the existence of an intermediate compound with composition $\text{Sb}_2\text{Te}_3 \cdot 2\text{InSb}$. On the left (l) and right (r) of this composition, the two parts of the dependence, $d_l(x)$ and $d_r(x)$, respectively, show smooth paths with positive convexity. This feature proves the existence of two homogeneity sub-areas [solid solutions based on the $\text{Sb}_2\text{Te}_3 \cdot 2\text{InSb}$ compound, i.e., $\text{Sb}_2\text{Te}_3 \cdot (2 + \delta)\text{InSb}$ ($-1 \leq \delta \leq +1$)].

The phase diagram of the Sb_2Te_3 -InSb system (Fig. 5) was built using the data obtained by DTA, XRD analysis, and H_V and d measurements.

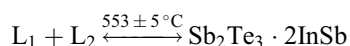
The phase diagram is complex and has the following peculiarities:

1. The incongruently melting intermediate compound $\text{Sb}_2\text{Te}_3 \cdot 2\text{InSb}$ is formed as a result of the syntectic reaction

Table 2 XRD structural data of the Sb₂Te₃:2InSb compound

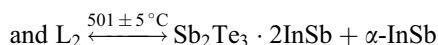
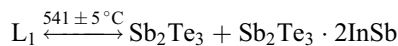
| No. | 2θ | θ | d _{exp} , Å | I | (I/I _{max})×100 (%) | Q = 1/d ² , Å ⁻² | hkl | d _c , Å |
|-----|-------|-------|----------------------|--------|-------------------------------|--|----------|--------------------|
| 1 | 20.20 | 10.10 | 4.3925 | 14.64 | 4 | 0.0518 | 100 | 4.3937 |
| 2 | 21.20 | 10.60 | 4.1875 | 57.38 | 16 | 0.0570 | 010 | 4.1963 |
| 3 | 25.16 | 12.58 | 3.5366 | 360.39 | 100 | 0.0800 | 001 | 3.5372 |
| 4 | 28.90 | 14.45 | 3.0869 | 193.69 | 54 | 0.1049 | 101 | 3.0346 |
| 5 | 38.88 | 19.44 | 2.3145 | 54.35 | 15 | 0.1867 | 111 | 2.3529 |
| 6 | 41.14 | 20.57 | 2.1924 | 93.86 | 26 | 0.2080 | 200 | 2.1969 |
| 7 | 42.90 | 21.45 | 2.1064 | 35.84 | 10 | 0.2254 | 020 | 2.0982 |
| 8 | 46.64 | 23.32 | 1.9459 | 247.56 | 69 | 0.2641 | 210, 210 | 1.9463 |
| 9 | 47.80 | 23.90 | 1.9013 | 258.14 | 72 | 0.2766 | 120 | 1.8933 |
| 10 | 48.44 | 24.34 | 1.8689 | 56.50 | 16 | 0.2863 | 201, 201 | 1.8662 |
| 11 | 49.12 | 24.56 | 1.8533 | 59.29 | 16 | 0.2911 | 021 | 1.8528 |
| 12 | 51.92 | 25.96 | 1.7597 | 31.79 | 9 | 0.3229 | 021 | 1.7599 |
| 13 | 59.52 | 29.76 | 1.5519 | 29.28 | 8 | 0.4152 | 220 | 1.5173 |
| 14 | 66.08 | 33.04 | 1.4128 | 40.03 | 11 | 0.5010 | 221 | 1.4163 |
| 15 | 71.52 | 35.76 | 1.3181 | 28.60 | 8 | 0.5756 | 022 | 1.3149 |
| 16 | 75.52 | 37.76 | 1.2579 | 74.36 | 21 | 0.6320 | 122 | 1.2597 |

Tetragonal lattice with parameters of $a = 4.3937 \text{ \AA}$, $b = 4.2035 \text{ \AA}$, $c = 3.5433 \text{ \AA}$, $\alpha = 93.354^\circ$, $\beta = \gamma = 90^\circ$; $\lambda = 1.5406 \text{ \AA}$

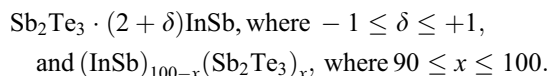


The stratification region, which lies on the syntectic horizontal, is limited by a monovariant curve with critical point at 570 °C. The existence of the Sb₂Te₃:2InSb compound was proved by XRD analysis and DTA, as well as by microhardness (H_V) and density (d) measurements.

- Two invariant eutectic equilibria exist in the Sb₂Te₃–InSb system with eutectic point coordinates at compositions of $x = 60$ and $x \approx 85$ mol% InSb and eutectic temperatures of $T_E = 541$ and $T_E \approx 501$ °C:



- A shift of the diffraction reflexes is observed at room temperature for both the intermediate compound Sb₂Te₃:2InSb (in the range from 50 to 75 mol% InSb) and InSb (in the range from 90 to 100 mol% InSb); i.e., limited solid solutions, based on Sb₂Te₃:2InSb and InSb (α -InSb), respectively, exist at this temperature in the concentration range of $50 \leq x \leq 75$ and $90 \leq x \leq 100$ mol% InSb. The exact record of these solid solutions is:



Their borders are proven by the XRD data and the dependence of H_V and d on the InSb concentration.

As a result of the complicated physicochemical interactions in liquid and solid state, one intermediate compound is

formed. This compound, together with the initial components Sb₂Te₃ and InSb, determines the existence of 10 phase fields, three of which are monophasic (I, V, and X) while the other seven are two-phase.

The unit cell parameters of the Sb₂Te₃:2InSb compound were determined by Ito's method^[39] (using XRD patterns taken at room temperature, 1000 h after synthesis).

The XRD data, the indexing results, and the unit cell parameters of the Sb₂Te₃:2InSb compound are presented in Table 2.

Analysis of the results obtained for the unit cell parameters (a, b, c and α, β, γ) shows that b and a , as well as α and β , differ insignificantly from each other, by $\sim -4.3\%$ and $\sim +3.7\%$ respectively; i.e., one can write $a \approx b \neq c$ and $\alpha \approx \beta = \gamma = 90^\circ$. These ratios between the unit cell parameters classify it as tetragonal. This means that, during the formation of the new tetragonal structure of Sb₂Te₃:2InSb, the component InSb tends to maintain angle equality ($\alpha = \beta = \gamma = 90^\circ$), while Sb₂Te₃ maintains the typical ratio of $a = b \neq c$ and $a \neq c$.

4. Conclusions

To study the phase equilibria in the Sb₂Te₃–InSb system, 17 samples with compositions in the interval 0–100 mol% InSb were prepared by a direct monotemperature method at maximal temperature of 700 ± 5 °C with synthesis duration at this temperature of 2 h.

Using four independent methods (XRD analysis, DTA, and density and microhardness measurements), the phase diagram of this system was built, being characterized by the following peculiarities:

- As a result of syntectic reaction occurring at temperature of 553 °C with participation of alloys containing

from ~62 to ~78 mol% InSb, an incongruently melting intermediate compound with composition $\text{Sb}_2\text{Te}_3\cdot 2\text{InSb}$ is formed. It is characterized by a wide homogeneity region extending from 50 to 75 mol% InSb at room temperature; i.e., the composition of the solid solution is $\text{Sb}_2\text{Te}_3\cdot(2 + \delta)\text{InSb}$, where $-1 \leq \delta \leq +1$.

- The $\text{Sb}_2\text{Te}_3\cdot 2\text{InSb}$ compound has tetragonal lattice with unit cell parameters of $a = 4.3937 \text{ \AA}$, $b = 4.2035 \text{ \AA}$, $c = 3.5433 \text{ \AA}$, $\alpha = 93.354^\circ$, and $\beta = \gamma = 90^\circ$.
- Boundary solid solutions based on InSb with composition $(\text{InSb})_{100-x}(\text{Sb}_2\text{Te}_3)_x$, where $90 \leq x \leq 100$, are also formed in the investigated system.
- Two invariant equilibria with eutectic temperatures of 541 and 501 °C and corresponding eutectic points at 60 and ~85 mol% InSb exist in the system.
- The initial components (Sb_2Te_3 and InSb) and the $\text{Sb}_2\text{Te}_3\cdot 2\text{InSb}$ compound determine the existence of 10 phase fields, three of which are monophasic while the other seven fields are two-phase.

Acknowledgment

This investigation has been financed by the Scientific Research Sector of the University of Chemical Technology and Metallurgy, Sofia, Bulgaria (Contract 11143). The authors express their gratitude for this support.

References

1. A.F. Ioffe, Energeticheskie osnovy termoelektricheskoi baterii iz poluprovodnikov, AN SSSR, Moskva-Leningrad, 1951 (in Russian)
2. A.F. Ioffe, Poluprovodnikovye termoelementy, AN SSSR, Moskva-Leningrad, 1960 (in Russian)
3. V.M. Glazov, A.S. Ohotin, R.P. Borovikova, and A.S. Pushkarskii, Metody issledovaniya termoelektricheskikh svoystv poluprovodnikov, Atomizdat, Moskva, 1969, p. 32 (in Russian)
4. L.I. Anatyichuk, Termoelementy i termoelektricheskie ustroystva, Spravochnik, Naukova dumka, Kiev, 1979 (in Russian)
5. F. Klein, Termoelektricheskie materialy i preobrazovatelei, Mir, Moskva, 1960, p 212 (in Russian)
6. T. Ikeda, E. Toberer, V.A. Ravi, G.J. Snyder, S. Aoyagi, E. Nishibori, and M. Sakata, In Situ Observation of Eutectoid Reaction Forming a $\text{PbTe-Sb}_2\text{Te}_3$ Thermoelectric Nanocomposite by Synchrotron X-Ray Diffraction, *Scr. Mater.*, 2009, **60**(5), p 321
7. T. Ikeda, S.M. Haile, V.A. Ravi, H. Azizgolshani, F.S. Gascoin, and G.J. Snyder, Solidification Processing of Alloys in the Pseudo-binary $\text{PbTe-Sb}_2\text{Te}_3$ System, *Acta Mater.*, 2007, **55**, p 1227
8. L.E. Shelimova, O.G. Karpinskii, T.E. Svechnikova, E.S. Avilov, M.A. Kretova, and V.S. Zemskov, Synthesis and Structure of Layered Compounds in the $\text{PbTe-Bi}_2\text{Te}_3$ and $\text{PbTe-Sb}_2\text{Te}_3$ Systems, *Inorg. Mater.*, 2004, **40**(12), p 1264
9. A. Thompson, J. Sharp, C.J. Rawn, and B.C. Chackoumakos, Structural Studies of GeTe-AgSbTe_2 Alloys, *Mater. Res. Soc. Symp. Proc.*, 2008, **1044**, p 3
10. L.E. Shelimova, T.E. Svechnikova, P.P. Konstantinov, O.G. Karpinskii, E.S. Avilov, M.A. Kretova, and V.S. Zemskov, The n- and p-Type Mixed Layered Tetradymite-Like Compounds with Low Lattice Thermal Conductivity: Growth, Structure and Thermoelectric, *Proc. 2nd Eur. Conf. on Thermoelectrics*, Krakov, 2004, p 202
11. L.E. Shelimova, T.E. Svechnikova, P.P. Konstantinov, O.G. Karpinskii, E.S. Avilov, M.A. Kretova, and V.S. Zemskov, Anisotropic Thermoelectric Properties of the Layered Compounds PbSb_2Te_4 and PbBi_4Te_7 , *Inorg. Mater.*, 2007, **43**(2), p 125
12. S.A. Nemov, M.K. Zhitinskaya, L.E. Shelimova, and T.E. Svechnikova, On the Hole Scattering Anisotropy in the PbSb_2Te_4 Layered Compound from Data on the Nernst-Ettingshausen Coefficient, *Phys. Solid State*, 2008, **50**(7), p 1215
13. M.K. Zhitinskaya, S.A. Nemov, L.E. Shelimova, T.E. Svechnikova, and P.P. Konstantinov, Thermopower Anisotropy in the Layered Compound PbSb_2Te_4 , *Phys. Solid State*, 2008, **50**(1), p 6
14. T. Ikeda, L.A. Collins, V.A. Ravi, F.S. Gascoin, and S.M. Haile, Self-Assembled Nanometer Lamellae of Thermoelectric PbTe and Sb_2Te_3 with Epitaxy-Like Interfaces, *J. Snyder Chem. Mater.*, 2007, **19**, p 763
15. L.E. Shelimova, O.G. Karpinskii, T.E. Svechnikova, I. Nikhezina, S. Avilov, M.A. Kretova, and V.S. Zemskov, Effect of Cadmium, Silver, and Tellurium Doping on the Properties of Single Crystals of the Layered Compounds PbBi_4Te_7 and PbSb_2Te_4 , *Inorg. Mater.*, 2008, **44**(12), p 371
16. J.H. Sun, X.Y. Xin, D. Li, L. Pan, C.J. Song, J. Zhang, R.R. Sun, Q.Q. Wang, and Y.F. Liu, Synthesis and Thermoelectric Properties of $\text{Zn}_4\text{Sb}_3/\text{Bi}_{0.5}\text{Sb}_{1.5}\text{Te}_3$ Bulk Nanocomposites, *J. Alloys Compd.*, 2010, **500**, p 215
17. L.V. Poreckaya, N.H. Abrikosov, and V.M. Glazov, Issledovanie sistemyi Sb-Te v oblasti soedineniya Sb_2Te_3 v tverdom i jidkom sostoianii, *J. Neorg. Himii*, **8**(5), 1963, p 1196 (in Russian)
18. N.H. Abrikosov, L.V. Poreckaya, and N.P. Ivanova, Issledovanie sistemyi surma-tellur, *J. Neorg. Himii*, **4**(11), 1959, p 2525 (in Russian)
19. M.A. Popescu, *Non-crystalline Chalcogenides*, Springer, New York, 2001
20. B.Yu. Yavorsky, N.F. Hinsche, I. Merig, and P. Zahn, Electronic Structure and Transport Anisotropy of Bi_2Te_3 and Sb_2Te_3 , *Phys. Rev. B*, 2011, **84**(165208), p 1
21. R. Jäschke, Elektrische Leitfähigkeit von Antimontellurid-Einkristallen (Halbleitereigenschaften von Telluriden. I), *Ann. Physik*, 1965, **15**(7), p 106 (in German)
22. D.A. Wright, *Research*, 1959, **12**(8-9), p 300
23. J. Black, E.M. Conwell, L. Seigle, and C.W. Spencer, Electrical and Optical Properties of Some $\text{M}_2^{y-b}\text{N}_3^{y-b}$ Semiconductors, *J. Phys. Chem. Sol.*, 1957, **2**(3), p 240
24. M.H. Benel, Propriétés thermoelectriques du tellurure d'antimoine et des solutions solides $\text{Sb}_2\text{Te}_3\text{-Bi}_2\text{Te}_3$, *Acad CR Sci.*, 1958, **247**, p 584 (in French)
25. V. Vassilev, Z. Boncheva-Mladenova, Himia i fizikohimia na poluprovodnicite, Univ. Izd. "Sv. Kl. Ohridski", Sofia, 2009 (in Bulgarian)
26. T.S. Liu and E.A. Peretti, *Trans. ASM*, 1952, **44**, p 539
27. J. Wooley and P. Keating, Solid Solubility of In_2Se_3 in Some Compounds of Zinc Blende Structure, *J. Less Common Met.*, 1961, **3**, p 194
28. International Centre of Diffraction Data, Joint Committee on Powder Diffraction Standards, Powder Diffraction File 06-0208
29. R. De Rider, J. De Sitter, and S. Amelinck., An Electron Microscopic Study of the Polymorphic Transformation in Ag_2Se II. The Structure of $\alpha\text{-Ag}_2\text{Se}$, *Phys. Stat. Sol.*, 1974, **23a**, p 615

30. E.S. Krupnikov, F.F. Aliev, and S.A. Aliev, Fazovie prehodii v teluride serebra, *Fizika Tverdogo Tela*, 1991, **33**(11), p 3408 **(in Russian)**
31. O. Madelung and H. Weiss, Die elektrischen Eigenschaften von Indium-antimonid II, *Z. Naturforschung*, 1954, **9a**, p 527 **(in German)**
32. G. Bush and E. Steigmaier, Wärmeleitfähigkeit, elektrische Leitfähigkeit, Hall-effekt und Thermospannung von InSb, *Helv. Phys. Acta*, 1960, **34**, p 1 **(in German)**
33. Ya.A. Ugai, Vvedenie v himiyu poluprovodnikov, Vysshaya shkola, Moskva, 1975 **(in Russian)**
34. S.S. Gorelik and M.Ya. Dashevskiy, Materialovedenie poluprovodnikov i metallov, Metallurgia, Moskva, 1973, p 488 **(in Russian)**
35. International Centre of Diffraction Data, Joint Committee on Powder Diffraction Standards, powder diffraction file 04-003-6722
36. International Centre of Diffraction Data, Joint Committee on Powder Diffraction Standards, powder diffraction file 03-065-9320
37. V. Vassilev, M. Radonova, E. Fidancevska, and S. Boycheva, Basic Physicochemical Properties of Glasses in the GeSe₂-Sb₂Te₃-CdSe System, *International Scientific Conference UNITECH'07, 23-24 November 2007, Gabrovo, Proceedings, II-365*
38. CRC Handbook of Chemistry and Physics, Internet version 2005, David R. Lide, ed., <http://www.hbcpnetbase.com>, CRC Press, Boca Raton, 2005
39. T. Ito, *X-ray Studies on Polymorphism*, Maruzen Co., Ltd., Tokyo, 1950, p 187